Scattering of nucleons from nuclei with couplings to particle-unstable excited states

P.R. Fraser[a,b,*], K. Amos[b], L. Canton[c], S. Karataglidis[d], J.P. Svenne[e], and D. van der Knijff[b]

[a] *Instituto de Ciencias Nucleares, Universidad Nacional Autónoma de México,*
México, D.F., 04510, Mexico.
e-mail: paul.fraser@nucleares.unam.mx
[b] *School of Physics, University of Melbourne,*
Victoria 3010, Australia.
[c] *Istituto Nazionale di Fisica Nucleare,*
Sezione di Padova, I-35131, Italy.
[d] *Department of Physics, University of Johannesburg,*
P.O. Box 524, Auckland Park, 2006, South Africa.
[e]*Department of Physics and Astronomy,University of Manitoba and*
Winnipeg Institute for Theoretical Physics, Winnipeg, MB, R3T 2N2, Canada.

The physics of radioactive ion beams implies the description of weakly-bound nuclear systems. One key aspect concerns the coupling to low-lying collective-type excited states, which for these systems might not be stable levels, but particle emitting resonances. In this work we describe how the scattering cross section and compound spectra change when the colliding fragments have such collective excitations featuring particle emission. We explore this question in the framework of a multi-channel algebraic scattering method of determining nucleon-nucleus cross sections at low energies. For a range of light-mass, particle-unstable nuclear targets, scattering cross sections as well as the spectra of the compound nuclei formed have been determined from calculations that do and do not consider particle emission widths for nuclear states. Assuming a resonance character for target states markedly varies evaluated cross sections from those obtained assuming the target spectrum to have entirely discrete states.

Keywords: Nuclear reactions; radioactive ion beams; neutron scattering; proton scattering; resonances.

La física de haces de iones radiactivos implica la descripción de sistemas nucleares débilmente ligados. Un aspecto clave de interés es el acoplamiento estados excitados de tipo colectivo yaciendo en niveles bajos, que para estos sistemas podrían no ser niveles estables, pero las partículas que emiten resonancias. En este trabajo se describe cómo la sección eficaz de dispersión y el cambio de espectros compuestos cuando los fragmentos que chocan tienen tales excitaciones colectivas caracterizando la emisión de partículas. Nosotros abordamos esta pregunta en el marco de un método de dispersión algebraíco multi-canal para determinar las secciones transversales nucleón-núcleo a bajas energías. Para un rango objetivos nucleares de partículas inestables livianas, las secciones transversales de dispersión, así como los espectros de los núcleos compuestos formados han sido determinados por los cálculos que consideran o no los anchos de emisión de partículas para los estados nucleares. Suponiendo un carácter resonante para los estados objetivos, las secciones transversales varían considerablemente de aquellas obtenidas suponiendo que el espectro objetivo tiene completamente estados discretos.

Descriptores: Reacciones nucleares; haces de iones radiactivos; dispersión de neutrones; dispersión de protones; resonancias.

PACS: 24.10.Eq; 24.30.-v; 25.40.-h; 25.60.-t

1. Introduction

The availability of radioactive ion beams (RIB) at many laboratories has given experimental information on many exotic nuclei. Those studies have revealed novel structures, such as nuclear skins and halos. Of particular interest are data obtained from scattering exotic nuclei from hydrogen targets, which equates in inverse kinematics to proton scattering from those nuclei. For incident energies of many tens of MeV per nucleon, such data have been analyzed in terms of effective nucleon-nucleus interactions used in distorted wave approximations [1-3]. For lower energies, at which the states in the low excitation regime of the target are influential, coupled-channels approaches [4,5] are needed. Coupled-channel analyses of RIB data made so far assumed scattering nuclei to

have spectra of discrete (zero-width) states. There has been a study of such systems at intermediate energies which sought to account for the low binding by including additional decay channels [6]. However, those authors did not consider decay widths for the nuclear states included in those coupled channels. Radioactive nuclei, and especially those near the drip lines, have quite low particle emission thresholds and thus can have low-lying resonance states in their spectra.

This paper considers nucleon scattering from a range of weakly-bound, light-mass nuclei, for which discrete resonance effects in the elastic cross section are present. Evaluations of both the scattering cross sections and of the spectra of the compound nucleus have been made using the development [7] in which particle emission widths are accounted for within a multi-channel algebraic scattering (MCAS) the-

ory [5]. With MCAS, solutions of coupled Lippmann-Schwinger equations are found (in momentum space) by using finite-rank separable representations of an input matrix of nucleon-nucleus interactions. The separable form factors are generated from a set of sturmian functions [8]. Those sturmian functions are generated from the same input matrix of interactions. Details are given in Refs. 5 and 9.

There are distinct advantages in using the MCAS method. It includes a prescription [5] that allows one to locate all compound-system resonance centroids and widths regardless of how narrow they may be. Further, by use of orthogonalizing pseudo-potentials (OPP) in generating the sturmians and solving the Lippmann-Schwinger equations, it is ensured that

the Pauli principle is not violated [9]. That is so even if a collective model is used to specify nucleon-nucleus interactions. The latter is of paramount importance for coupled-channel calculations [10], as otherwise some compound nucleus wave functions so defined possess spurious components.

MCAS has been used previously to characterize scattering from nuclei away from the valley of stability [11,12], but in those studies, the target nuclei states were all taken to be of zero width. In this study, several of those previous investigations are amended to include particle-unstable channel widths.

In Sec. 2, a brief description is given of the MCAS method and how resonant character of a target state effects it. Then in Secs. 3 through 7, examples are described and results presented. A discussion is given, and conclusions drawn, in Sec. 8.

2. Theoretical development

The MCAS method was developed to find solutions of coupled-channel, partial-wave expanded Lippmann-Schwinger equations for nucleon-nucleus scattering. Details are given Ref. 5. This method leads to an algebraic representation of the scattering matrix

$$S_{cc'} = \delta_{cc'} - i^{(l_{c'}-l_c+1)}\pi\mu \sum_{n,n'=1}^{N} \sqrt{k_c}\hat{\chi}_{cn}(k_c)\left([\eta - \mathbf{G}_0]^{-1}\right)_{nn'}\hat{\chi}_{c'n'}(k_{c'})\sqrt{k_{c'}}. \tag{1}$$

The factor μ is $2m_{red}/\hbar^2$, m_{red} being the reduced mass. The indices c and c' refer to open channels, l_c is the partial wave in channel c and the Green's function matrix is

$$[\mathbf{G}_0]_{nn'} = \mu\left[\sum_{c=1}^{open}\int_0^\infty \hat{\chi}_{cn}(x)\frac{x^2}{k_c^2 - x^2 + i\varepsilon}\hat{\chi}_{cn'}(x)\,dx - \sum_{c=1}^{closed}\int_0^\infty \hat{\chi}_{cn}(x)\frac{x^2}{h_c^2 + x^2}\hat{\chi}_{cn'}(x)\,dx\right]. \tag{2}$$

Here, η is a column vector of sturmian [13] eigenvalues and $\hat{\chi}$ are form factors determined from the chosen sturmian functions.

Traditionally, all target states are taken to have eigenvalues of zero width, and the (complex) Green's functions are evaluated using the method of principal parts. However, if states decay, the Green's function matrix elements become

$$[\mathbf{G}_0]_{nn'} = \mu\left[\sum_{c=1}^{open}\int_0^\infty \hat{\chi}_{cn}(x)\frac{x^2}{k_c^2 - x^2 + \frac{i\mu\Gamma_c}{2}}\hat{\chi}_{cn'}(x)dx - \sum_{c=1}^{closed}\int_0^\infty \hat{\chi}_{cn}(x)\frac{x^2}{h_c^2 + x^2 - \frac{i\mu\Gamma_c}{2}}\hat{\chi}_{cn'}(x)dx\right], \tag{3}$$

where Γ is the width of the target state associated with channel c. With poles moved significantly off the real axis, direct integration of a complex integrand along the real momentum axis is feasible. This has been done. However, for any infinitesimal-width target state, or resonance so narrow that it can be treated as such, the method of principal parts has been retained.

An additional complication arises from the Lorentzian shape of target resonances as modeled by MCAS. Below threshold ($E = 0$), resonance (target state) widths must not cause instability for any compound system that has subthreshold states. To ensure this, an energy dependent scaling factor must be applied to target resonance states. As a first, minimal correction, this investigation applies a Heaviside step function, $H(E)$, at $E = 0$, forcing the target state spread to vanish below threshold. Eq. (3) then becomes

$$[\mathbf{G}_0]_{nn'} = H(E)\cdot\mu\left[\sum_{c=1}^{open}\int_0^\infty \hat{\chi}_{cn}(x)\frac{x^2}{k_c^2 - x^2 + \frac{i\mu\Gamma_c}{2}}\hat{\chi}_{cn'}(x)dx - \sum_{c=1}^{closed}\int_0^\infty \hat{\chi}_{cn}(x)\frac{x^2}{h_c^2 + x^2 - \frac{i\mu\Gamma_c}{2}}\hat{\chi}_{cn'}(x)dx\right]$$

$$+ (1 - H(E))\cdot\mu\left[-\sum_c\int_0^\infty \hat{\chi}_{cn}(x)\frac{x^2}{h_c^2 + x^2}\hat{\chi}_{cn'}(x)dx\right]. \tag{4}$$

TABLE I. Parameter values defining the nucleon-^{8}Be interaction.

	Odd parity	Even parity	
V_{central} (MeV)	-31.5	-42.2	
V_{ll} (MeV)	2.0	0.0	
V_{ls} (MeV)	12.0	11.0	
V_{ss} (MeV)	-2.0	0.0	
Geometry	$R_0 = 2.7$ fm	$a = 0.65$ fm	$\beta_2 = 0.7$
Coulomb†	$R_c = 1.3$ fm	$a_c = 1.00$ fm	$\beta_2 = 0.7$
	$0s_{1/2}$	$0p_{3/2}$	
0^+ $\lambda^{(OPP)}$	1000	0.0	
2^+ $\lambda^{(OPP)}$	2.0	0.2	
4^+ $\lambda^{(OPP)}$	0.0	0.0	

† for proton-^{8}Be calculations (see Section **??**).

In practice, however, this is not sufficient, as reaction cross sections approaching threshold increase asymptotically (see Sec. 3). More sophisticated methods to address this issue are in development, and indeed, one aim of this paper is to emphasize the need for such improvement.

3. $n+^8$Be scattering

The low-excitation ^{8}Be spectrum has a 0^+; 0 ground state that has a small width for decay into two α-particles (6×10^{-6} MeV), a broad 2^+; 0 resonance state with centroid at 3.03 MeV and width of 1.5 MeV, followed by a broader 4^+; 0 resonance state with centroid at 11.35 MeV and width ~ 3.5 MeV [14], both of which also decay into α-particles. As the width of the ground state is so small, it is approximated to be a zero-width state in our MCAS calculations.

Two evaluations of the $n+^8$Be cross section have been obtained with MCAS. In the first, both the 2^+ and 4^+ states were also taken to have zero-width and, as will be used throughout, results from such calculations are identified by the label 'no-width(s)'. In the second calculation, the true widths as tabulated [14] were used and results of such hereafter are identified by the label 'width(s)'. In both calculations, the same nuclear interaction was used. It was specified from a collective model of the nucleus with rotor character [5]. The parameter values used were chosen to give a fit to the low lying spectrum of ^{9}Be, and they are listed in Table I. They differ from those used in the previously published calculations [7], as some aspects of the experimentally determined structure of ^{9}Be are better reproduced. The spectra from the two calculations are depicted in Fig. 1. While some disparities remain, to be expected from the simple prescription we have used to specify the interaction potentials, compared to the previous results [7] the centroid energy of the $\frac{1}{2}^+$ first resonance is now placed above threshold in the widths case (see later regarding the degeneracy), and there are now no spurious states in the 0 to 5.5 MeV projectile energy range. The definition of all parameters can be found in
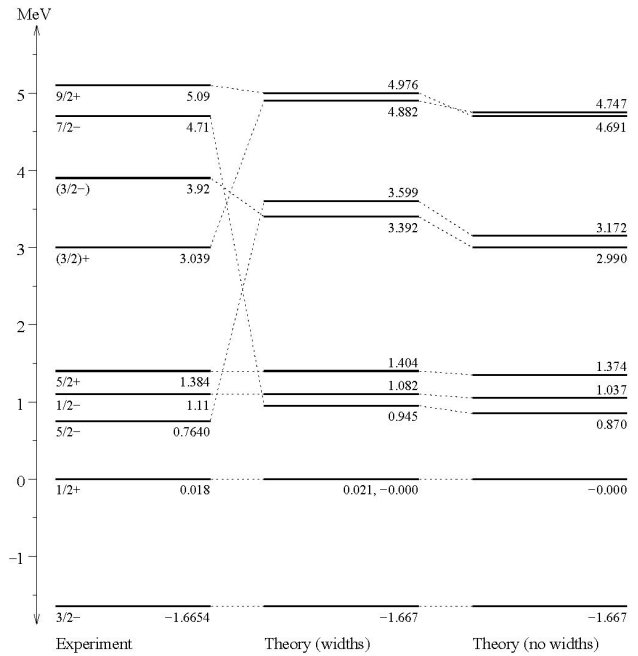

FIGURE 1. The experimental ^{9}Be spectrum and those calculated from MCAS evaluations of the neutron+^{8}Be system assuming the ^{8}Be states are resonances (widths) or are discrete (no widths).
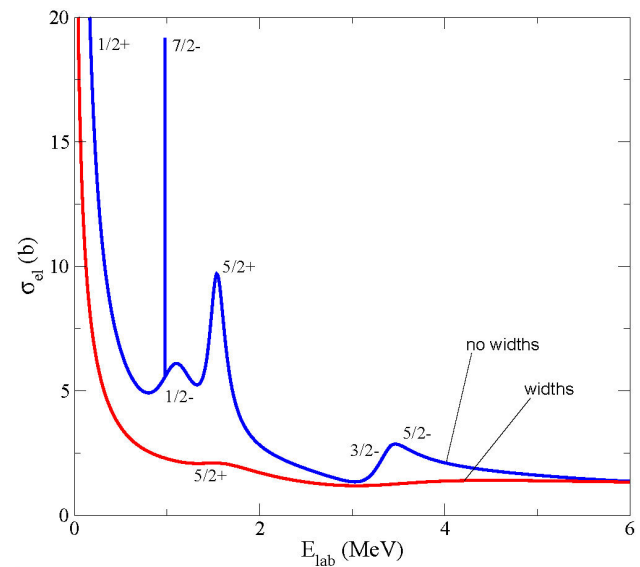

FIGURE 2. (Color online) Calculated cross sections for neutron scattering from ^{8}Be found using MCAS with and without the resonance character in the target states.

Ref. 5, with the addition of values for Pauli hindrance for the $0s_{1/2}$ and $0p_{3/2}$ subshells of the target states, as defined in Ref. 11 and 12.

Note that the $\frac{1}{2}^+$ state is naturally moved from the positive to negative regime with the removal of widths. Thus, the application of the Heaviside function means that in the widths case there are two representations of this state; the one frozen below zero and that moved above zero. This phenomenon is further discussed in Sec. VI.

TABLE II. Widths of states in ^{9}Be state widths (Γ in MeV). In order, the columns designate the state spin-parity, the experimental values, the MCAS no-width calculation results, ratios $\Gamma_{th} : \Gamma_{exp}$, the MCAS width calculation results, and ratios $\Gamma_{th} : \Gamma_{exp}$

J^π	$\Gamma_{exp.}$	$\Gamma_{no-width}$	$\frac{\Gamma_{no-width}}{\Gamma_{exp.}}$	Γ_{width}	$\frac{\Gamma_{width}}{\Gamma_{exp.}}$
$\frac{1}{2}^+$	0.217 ± 0.001	—	—	1.595	7.350
$\frac{7}{2}^-$	1.210 ± 0.230	2.08×10^{-5}	1.72×10^{-5}	1.641	**1.356**
$\frac{1}{2}^-$	1.080 ± 0.110	0.495	**0.458**	1.686	**1.561**
$\frac{5}{2}^+$	0.282 ± 0.011	0.187	**0.663**	0.740	**2.624**
$\frac{3}{2}^-$	1.330 ± 0.360	0.466	**0.350**	3.109	**2.337**
$\frac{5}{2}^-$	7.8×10^{-4}	0.060	76.74	2.772	3554
$\frac{9}{2}^+$	1.330 ± 0.090	0.386	0.290	2.498	**1.878**
$\frac{3}{2}^+$	0.743 ± 0.055	3.286	4.423	5.162	6.947

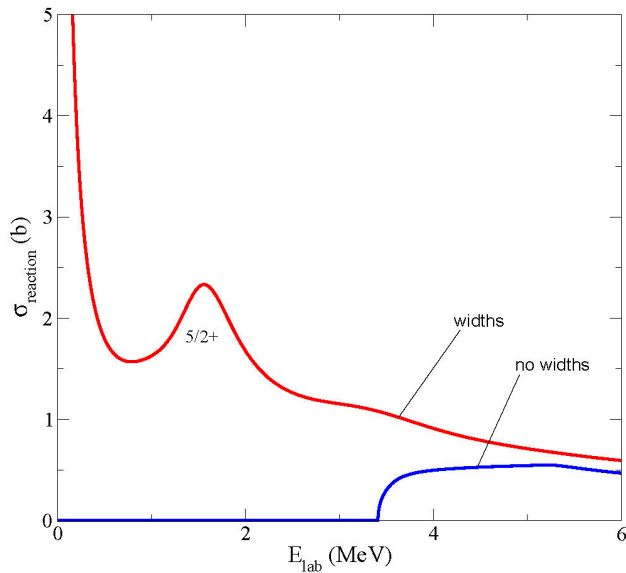FIGURE 3. (Color online) Reaction cross sections for n-^{8}Be scattering from the two MCAS (widths and no widths) calculations.

The results for the scattering cross sections are shown in Fig. 2. Upon introducing target-state widths, as found previously [7], the resonances linked to spectral properties of ^{9}Be are suppressed. They are still present but their widths have increased and their magnitudes decreased so as only the $\frac{5}{2}^+$, and arguably the $\frac{5}{2}^-$, can be discerned from the background. Low energy compound system resonances from both calculations are at essentially the same energies. Though as energy increases, the centroid energies found from the (target state) width calculation become increasingly higher than that of the no-width calculation.

Table II summarizes results. For each spin-parity (column 1), the listed experimental ^{9}Be resonance widths are given in column 2. They are compared with predicted values for neutron emission from the no-width (column 3) and width (column 5) calculations. In columns 4 and 6 the ratios

of the calculated widths to experiment are given. Boldface entries highlight the matches we find between theory and experiment to within a factor of 3.

Allowing the two excited states of ^{8}Be to be resonances gives the same spectral list as when they are treated as discrete, but the evaluated widths of resonances in the compound nucleus significantly increase. This is reflected in the cross sections. In the no-width case, narrow and broad resonances are evident but most melt into the background when the target states are allowed their widths. Where the no-widths case resonances are often overly narrow, the width case results are overly broad. While most of the theoretical ^{9}Be resonance widths given from the width calculation are closer, often significantly, to experimental values, a few are not.

From Fig. 2 it seems that the cross section background decreases in value with application of target state widths. The cause of this reduction in cross section magnitude is the loss of flux inherent with complex energies of the target states. That is illustrated by the reaction cross section of the $n+^8$Be scattering, shown in Fig. 3. The reaction cross section found in the no-width case is zero until 3.4 MeV (3.03 in the centre of mass frame), the first inelastic threshold. However, for the width case, with the direct integration method, there is a complex term in Eq. (4) for all positive values of projectile energy. Thus, the target state width method cross section has flux loss from zero projectile energy upwards. There is an asymptotic behaviour as energy approaches zero (see Sec. 2). While this could be attributed to the presence of the $\frac{1}{2}^+$
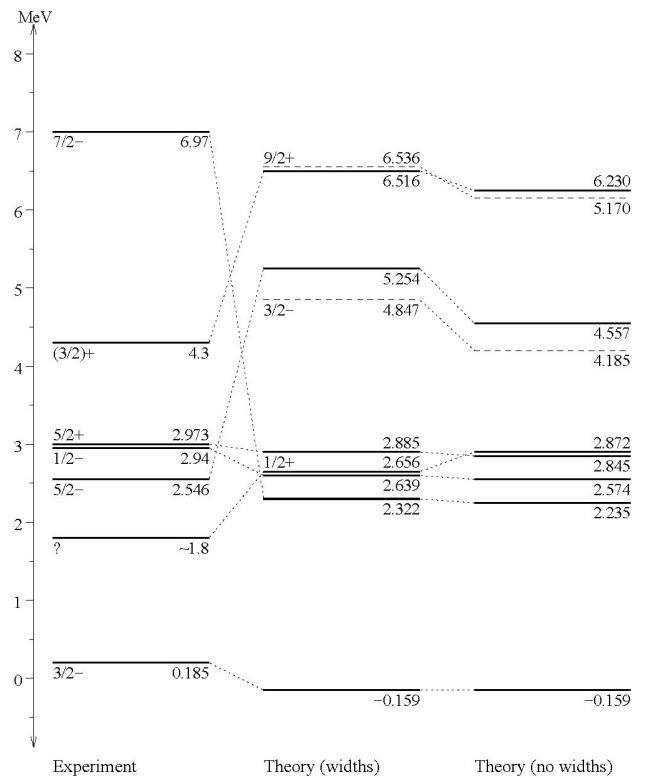

FIGURE 4. Experimental ^{9}B spectrum and the (widths and no widths) MCAS results for the $p+^8$Be system.

TABLE III. Widths of ^{9}B states (Γ in MeV). In order the columns contain the spin-parity of the state, the the experimental width, those from a no-width MCAS calculation, the ratios $\Gamma_{th} : \Gamma_{exp}$, those from a width MCAS calculation, and ratios $\Gamma_{th} : \Gamma_{exp}$.

J^π	$\Gamma_{exp.}$	$\Gamma_{no-width}$	$\frac{\Gamma_{no-width}}{\Gamma_{exp.}}$	Γ_{width}	$\frac{\Gamma_{width}}{\Gamma_{exp.}}$
$\frac{7}{2}^-$	2.0 ± 0.20	1.56×10^{-4}	7.78×10^{-4}	1.645	**0.82**
$\frac{1}{2}^-$	3.13 ± 0.02	0.652	0.21	2.087	**0.67**
$\frac{5}{2}^+$	0.55 ± 0.04	0.450	**0.82**	1.085	**1.97**
$\frac{1}{2}^+$	—	6.186	—	7.627	—
$\frac{3}{2}^-$	N/A	1.133	N/A	5.074	N/A
$\frac{5}{2}^-$	0.081 ± 0.005	0.887	10.954	5.024	62
$\frac{9}{2}^+$	N/A	0.837	N/A	3.169	N/A
$\frac{3}{2}^+$	1.6 ± 0.20	2.666	**1.666**	5.053	3.2

TABLE IV. Parameter values defining the nucleon-^{14}O interaction.

	Odd parity	Even parity
$V_{central}$ (MeV)	-44.2	-44.2
V_{ll} (MeV)	0.42	0.42
V_{ls} (MeV)	7.0	7.0
V_{ss} (MeV)	0.0	0.0
Geometry	$R_0 = 3.1$ fm $a = 0.65$ fm	$\beta_2 = -0.5$
Coulomb	$R_c = 3.1$ fm	

	$0s_{1/2}$	$0p_{3/2}$	$0p_{1/2}$
0^+ $\lambda^{(OPP)}$	1000	1000	1000
2^+ $\lambda^{(OPP)}$	1000	1000	3.11
4^+ $\lambda^{(OPP)}$	1000	1000	3.87

first resonance just above threshold, this behaviour was also observed in the work of Sec. VII, where no such low lying resonance exists.

In the reaction cross section from the width calculation, there is a broad peak at 1.5 MeV, corresponding to the $\frac{5}{2}^+$ resonance. This suggests that there is more flux loss at energies corresponding to compound system eigenstates than in the regions in between. There is also a broad, short bump at 3.4 MeV, but it is not clear how much loss of flux arises from the opening of the second inelastic channel, as this region also contains the theoretically broad $\frac{5}{2}^-$ resonance.

4. $p+^8$Be scattering

As a further investigation into this phenomenon, we have used nuclear interactions selected for neutrons on ^{8}Be (Table I) in calculations of the scattering with protons. The Coulomb potential used is that of the same deformed rotor and Woods-Saxon form, but with a Coulomb radius of 1.3 fm, and a deformation, β_2, of 0.7.

The experimental spectrum of the compound system, ^{9}B, is compared with theoretical spectra from width and no-width calculations as indicated in Fig. 4.

The observed states up to 8 MeV are matched by the calculated results, albeit in a few cases severely over- or underbound. As the observed spectral list replicates that of its mirror, ^{9}Be, a spin-parity, J^π, of $\frac{1}{2}^+$ is ascribed to the unknown state at ~1.8 MeV excitation. Likewise the unknown state at 4.3 MeV can be assigned the J^π of $\frac{3}{2}^+$. There are also two predicted states that are as yet unobserved.

As with the $n+^8$Be investigations, allowing the target states to have widths alters the centroid energies of the compound system. Again the centroids of the resonances are increased in comparison to their counterpart found from the no-width calculation. This effect increases with energy, with the exception of the state designated as $\frac{1}{2}^+$.

Table III summarizes resonance width results for the no-width and width calculations of ^{9}B. The columns are as

designated in Table II. Dashed entries indicate incomplete experimental data, and those marked N/A indicate states not seen experimentally. Again the cases of agreement to within a factor of 3 are highlighted.

Application of target states with widths yields a better match between the theoretical and experimental ^{9}B resonance widths for the $\frac{7}{2}^-$ and $\frac{1}{2}^-$ cases, but slightly worse results for the $\frac{5}{2}^+$ and $\frac{3}{2}^+$ resonances. However, the $\frac{3}{2}^+$ does not agree well with the known centroid energy, as is the case with the most poorly predicted resonance, the $\frac{5}{2}^-$. Again these are limitations such as one must expect on using a simple model for the nuclear interactions.

5. $p+^{14}$O scattering

The low excitation spectrum of ^{14}O has a $0^+; 1$ ground state with a small width for β^+ decay ($\tau = 70.606 \pm 0.018s$), followed by a band starting 0.545 MeV above the proton-^{13}N threshold and consisting of a $1^-; 1$ state at 5.173 MeV, and then known proton-unstable resonances with spin-parities of $0^+; 1$ at 5.920 MeV (decay width of ≤0.05 MeV), of $3^-; 1$ at 6.272 MeV (decay width of 0.103 MeV), and of $2^+; 1$ at 6.590 MeV (decay width of ≤0.06 MeV) [14].

To investigate the sensitivity of scattering observables to such small particle-decay widths, two evaluations of the $p+^{14}$O resonance spectrum were made. Again, in both, the ground state was taken to be zero-width. Of the low energy spectrum, the 0_2^+ and 2^+ were selected for coupling in a previous study, as in the mirror $n+^{14}$C system they generated the low-energy negative-parity states in ^{15}C [11]. In the first calculation, both are taken as zero-width (ignoring their known proton-decay widths) while in the second, the upper limits of the known widths were used. In both calculations, the same nuclear interaction was used and it was generated assuming the collective model with rotor character for the structure. The parameter values were chosen to be those used in a previous paper [11] (and shown here for comparison with the new widths calculation), and as such are fitted for the no-width
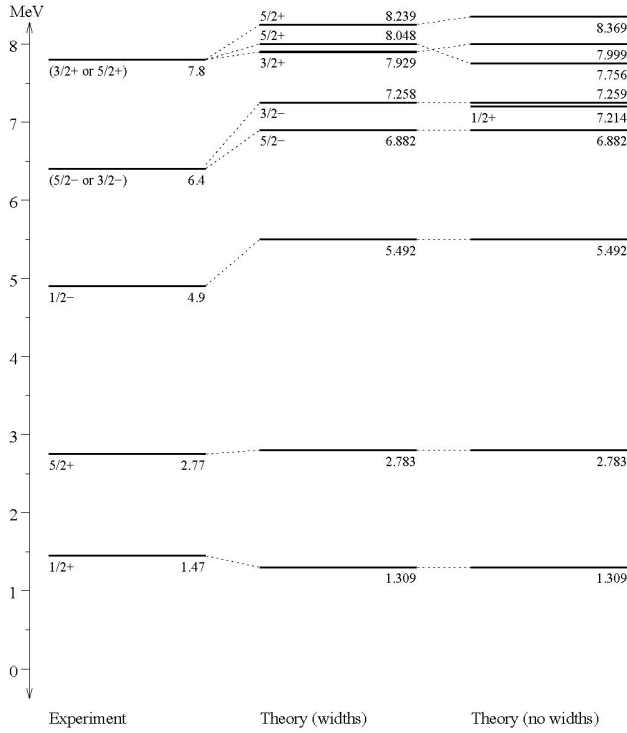
FIGURE 5. Experimental ^{15}F spectrum and those from MCAS (widths and no widths) calculations of the $p+^{14}$O system.

case. For completeness, these are given in Table IV. In this case, the proton distribution is taken as that of a uniformly charged sphere of radius 3.1 fm.

The compound system, ^{15}F is particle unstable and only its ground and first excited resonance states were known until recently [15]. Definite spin-parity assignments have been made for the lowest three experimentally known states while the fourth and fifth given in Ref. 15, tentatively are $\frac{3}{2}^-$ or $\frac{5}{2}^-$ for the 6.4 MeV state and $\frac{3}{2}^+$ or $\frac{5}{2}^+$ for the 7.8 MeV state. These resonance state centroids are compared with the spectra predicted from our MCAS calculations in Fig. 5. The measured states pair up quite reasonably with the calculated ones. There is a close agreement with the centroids of the theoretical resonances save for one. Why the $\frac{1}{2}^+$ of the no-width calculation has no matching partner in the spectrum from the width calculation is unknown at this time.

It should be noted that the parameters that produced this spectrum were fitted only to the observed $\frac{1}{2}^+$ and $\frac{5}{2}^+$ states, before the results of Ref. 15 were published, highlighting the strength of the previously-published no-widths calculation, and the predictive power of the MCAS method.

The ^{15}F resonance width results for the no-width and width calculations are in comparison with the known values in Table V. The columns are as per Table II. Both calculations give good agreement (to within the factor of 3 used as a measure) as is indicated by favourable ratios being displayed in boldface.

The two predicted resonances that may correspond to the fourth observed state increase in width when target state widths areintroduced, bringing them closer to the experimen-

TABLE V. ^{15}F state widths (Γ in MeV) from experiment, calculation with ^{14}O states taken as zero-width, ratios $\Gamma_{\text{th.}} : \Gamma_{\text{exp.}}$, calculation with ^{14}O states taken with known width, and ratios $\Gamma_{\text{th.}} : \Gamma_{\text{exp.}}$.

J^π	$\Gamma_{exp.}$	$\Gamma_{no-width}$	$\frac{\Gamma_{no-width}}{\Gamma_{exp.}}$	Γ_{width}	$\frac{\Gamma_{width}}{\Gamma_{exp.}}$
$\frac{1}{2}^+$	1.00 ± 0.20	0.77	**0.77**	0.77	**0.77**
$\frac{5}{2}^+$	0.24 ± 0.03	0.30	**1.25**	0.32	**1.33**
$\frac{1}{2}^-$	0.2 ± 0.20	4.22×10^{-3}	47	5.43×10^{-2}	3.68
$(\frac{5}{2}^-)$	0.2 ± 0.20	0.01	0.05	0.07	**0.35**
$(\frac{3}{2}^-)$	0.2 ± 0.20	3.68×10^{-2}	0.18	0.09	**0.45**
$(\frac{3}{2}^+)$	0.4 ± 0.40	3.67	9.19	0.16	**0.4**
$(\frac{5}{2}^+)$	0.4 ± 0.40	0.42	**1.05**	0.07	0.18
$(\frac{5}{2}^+)$	0.4 ± 0.40	0.55	**1.38**	0.24	**0.61**

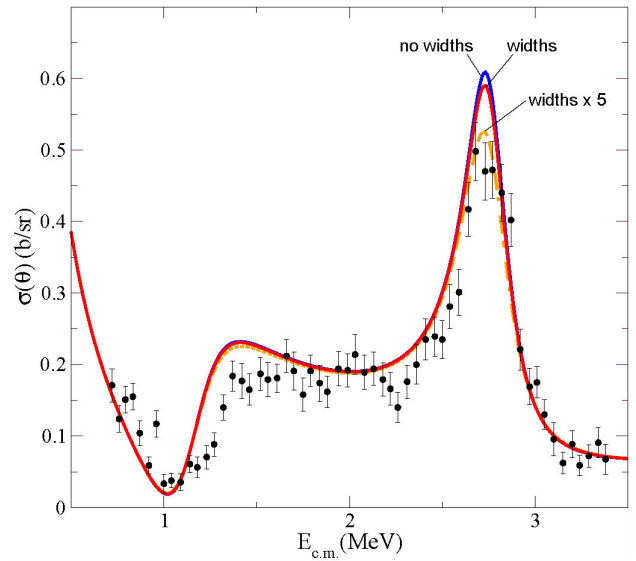

FIGURE 6. (Color online) MCAS calculated elastic cross sections for $p+^{14}$O scattering at $147°$ scattering angle compared with experimental data [16]. Details are given in the text.
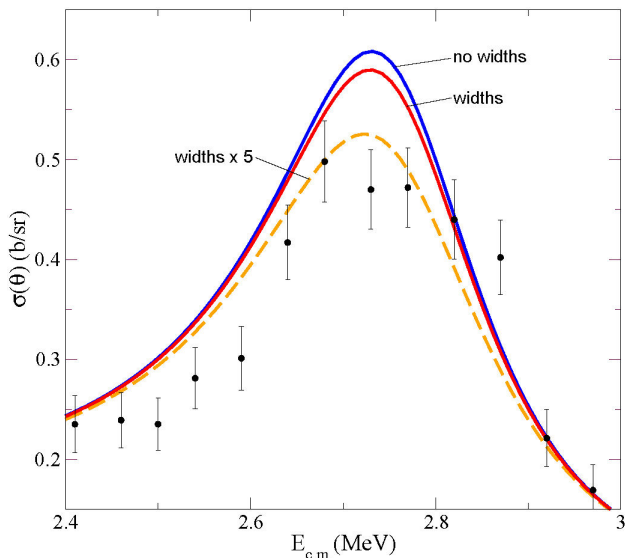
tal value in Ref. 15, in line with comments in that paper. However, the three predicted resonances that may correspond to the fifth observed state decrease in width when target state widths are introduced, bringing the $\frac{3}{2}^+$ resonance closer to the observed value, but taking the second of the two $\frac{5}{2}^+$ resonances outside of the factor of 3 used as a measure of quality.

More telling, however, is the comparisons of calculated results with $p+^{14}$O cross sections. Scattering of low energy ^{14}O ions from hydrogen targets has been measured [16], and a comparison of our calculated cross sections with their data taken at a scattering angle of $147°$ is made in Fig. 6.
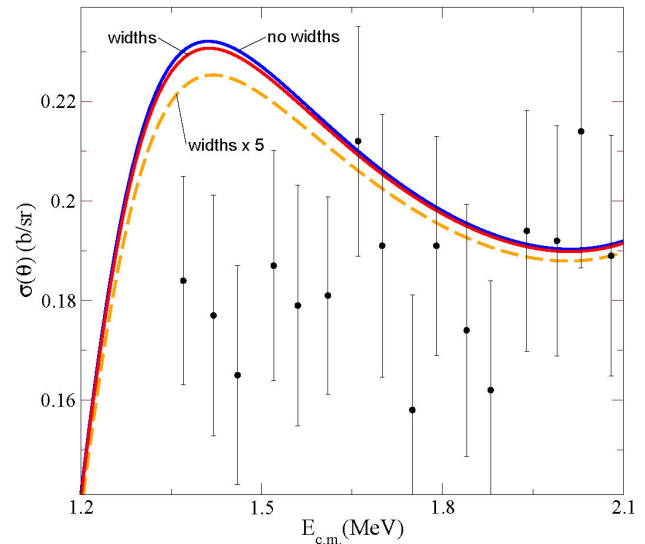
Clearly both calculations give very good results, with obvious evidence of the effect of the two resonances in the compound system. Inclusion of experimental decay widths of the target states, in this case, does not obviously improve the comparison with the data in this figure. However, there is a little improvement in the energy variation of the results over

TABLE VI. Parameter values defining the nucleon-^{6}He interaction.

	Odd parity	Even parity
V_{central} (MeV)	-36.8177	—
V_{ll} (MeV)	-1.2346	—
V_{ls} (MeV)	14.9618	—
V_{ss} (MeV)	0.8511	—

Geometry	$R_0 = 2.8$ fm	$a = 0.88917$ fm	$\beta_2 = 0.7298$
Coulomb	$R_c = 2.0$ fm		

Proton blocking	$0s_{1/2}$	$0p_{3/2}$	$0p_{1/2}$
0^+ $\lambda^{(OPP)}$	1000	0.0	0.0
2_1^+ $\lambda^{(OPP)}$	1000	0.0	0.0
2_2^+ $\lambda^{(OPP)}$	1000	0.0	0.0
Neutron blocking	$0s_{1/2}$	$0p_{3/2}$	$0p_{1/2}$
0^+ $\lambda^{(OPP)}$	1000	17.8	36.0
2_1^+ $\lambda^{(OPP)}$	1000	17.8	5.8
2_2^+ $\lambda^{(OPP)}$	1000	17.8	5.8

FIGURE 8. (Color online) Calculated elastic cross sections for $p+^{14}$O scattering at $147°$ scattering angle for energies centred on the $\frac{1}{2}^+$ resonance compared with the experimental data [16].

6. $p+^6$He system

To study the effect of target state particle-emission widths on calculated resonance centroids over a large range of projectile energies, the $p+^6$He system is examined. The known spectrum of the compound system, ^{7}Li, is particularly well suited to this as it has known states over a 15 MeV interval. As most of these compound system states lie below the $p+^6$He threshold, the Heaviside function discussed in Sec. 2 has not been used. The aim here is not to produce cross sections, but to study effects of target state widths on the compound nucleus spectrum.

The low excitation spectrum of ^{6}He consists of a 0^+; 1 ground state with a very small width ($\tau = 806.7 \pm 1.5 ms$) for β^- emission, followed by a 2^+; 1 state at 1.797 MeV of width 0.113±0.02 MeV which emits neutrons and α-particles, followed, at 5.6 MeV, by a degenerate triplet designated $(2^+, 1^-, 0^+)$; 1 with a width of 12.1±1.1 MeV. The decay paths of this triplet are unknown, though particle instability can be assumed.

Two evaluations of the $p+^6$He compound system were obtained with MCAS; in both, the ground state was taken as having zero-width. In the first calculation the excited states were also assumed to have zero-width. In the second, the true width of the 2_1^+ evaluated from reaction data was used, and the full width of the triplet, $(2^+, 1^-, 0^+)$; 1 was ascribed to the 2_2^+ state. In both calculations, the same nuclear interaction was considered, again taken from a collective model with rotor character [5] using the parameter values of Ref. 12. They were determined by a no-width calculation of the ^{7}Li spectrum (and shown here for comparison with the new widths calculation). For completeness, they are listed in Table VI. The known compound-system spectrum [14] contains only negative parity states, and thus there is no guide for
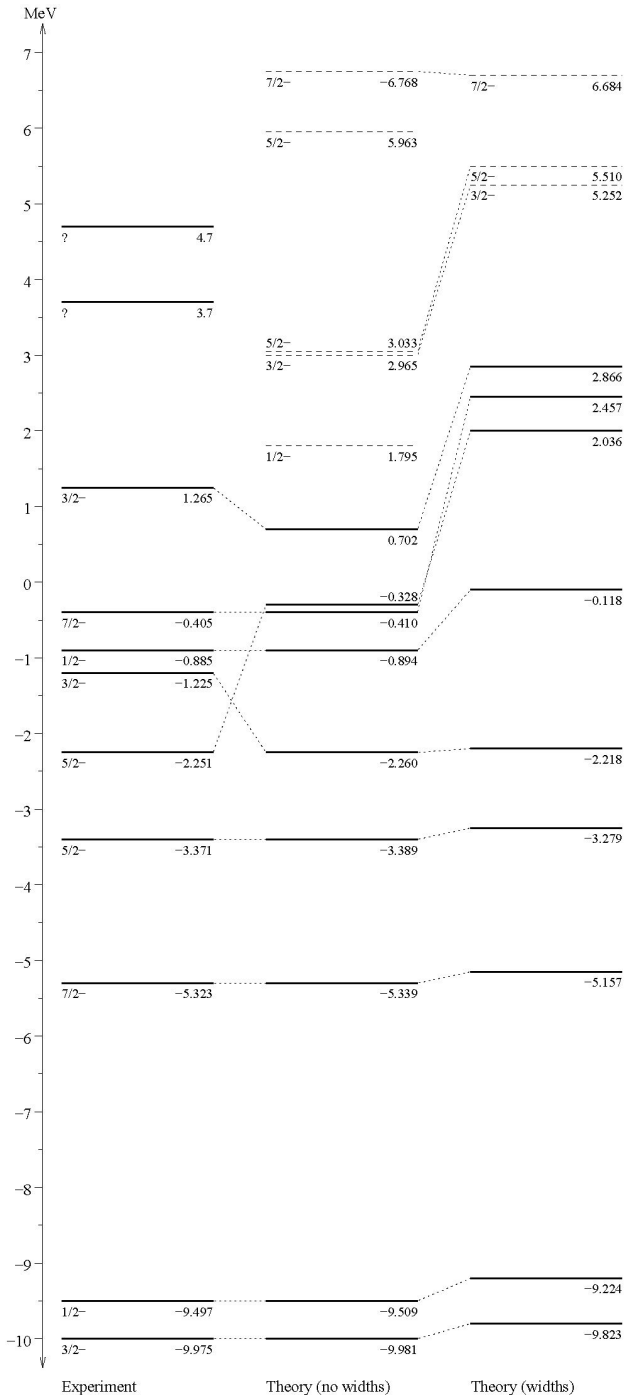

FIGURE 7. (Color online) Calculated elastic cross sections for $p+^{14}$O scattering at $147°$ scattering angle for energies centred on the $\frac{5}{2}^+$ resonance compared with the experimental data [16].

the ^{15}F resonance regions, where the no-width calculations had larger value than experiment. The cross sections for just those energy regions are shown in Figs. 7 and 8. The improvements are slight but in the correct direction. For comparison, a cross section for a hypothetical case in which the target state widths are five times larger than observed is displayed by the dashed line in Figs. 6, 7, and 8. At this stage, experimental data of higher accuracy is most desirable, to ascertain these fine details.

FIGURE 9. Experimental ^{7}Li spectrum and those from (no widths and widths) MCAS calculations of the $p+^6$He system.

fitting positive-parity parameters. Thus, positive parity interactions are not considered. The proton distribution was taken as a uniform charged sphere. The actual known spectrum of the compound system, ^{7}Li, and the theoretical spectra found from our two MCAS evaluations are displayed in Fig. 9. The reference energy is the $p+^6$He threshold and so all states below that energy in ^{7}Li are discrete in so far as proton emission is concerned. There are other thresholds for particle emission lying below this value and so many are res-

onances in their own right. For example the ^{3}He$+\alpha$ threshold is at 2.467 MeV so that the set of states lying between the $\frac{7}{2}^-$ ones are resonances with regard to that break-up. MCAS studies have been made to note such [12], though since the two nuclei involved have no excited states of import that was a single channel study.

As the parameters are fitted to the no-width case, in this case, that spectrum is shown next to the data. Note, these results for the calculation without target state widths are marginally different from those in Ref. 12, by at most 18 eV, as the program suite has undergone many small refinements since that publication.

The differences between these calculated spectra suggest that, as projectile energy increases, the consideration of the target state widths increasingly shifts the energy levels from the values found from the no-width calculation. Overall, the energy levels (and resonance centroids) increase as the excitation energy increases compared to the no-width results, similar to what was observed with the ^{8}Be investigations. In addition, there are two resonances in the spectrum found in the no-width case that are missing in the results found from the width calculation. They are the $\frac{1}{2}^-$ (1.795 MeV) and $\frac{5}{2}^-$ (5.963 MeV) resonances. Also there is a $\frac{7}{2}^-$ resonance (2.457 MeV) only found in the width results. Of the resonances above the $p+^6$He threshold that MCAS predicts, only one is matched to an observed state with definite J^π, the $\frac{3}{2}^-$ at 1.265 MeV. No comparison is drawn between the matches of predicted widths to observation, as it is poorly recreated in centroid in both calculation.

Note that, as with the $\frac{1}{2}^+$ state in Sec. 3, the $\frac{5}{2}^-_2$ and $\frac{7}{2}^-_2$ states are naturally moved from the negative to the positive energy regime with the application of widths. Thus, the application of the Heaviside function would mean there would be two representations of this state; one in which it is a subthreshold state and the other in which it is a resonance. However, as noted in Sec. 4, occasionally the reverse occurs. This is an additional indication that another method is required to prevent width-penetration into the negative energy regime, one which localizes the effects of widths of target states to the region surrounding their centroids.

Comparisons between the matches of predicted widths to observation for the higher excitations are not good with either of the calculations. Improved MCAS studies are needed.

7. $n+^6$He system

To investigate further the asymptotic increase in reaction cross section as projectile energy approaches zero, the $n+^6$He system was investigated. The nuclear interaction was set as that given in Table VI, with neutron Pauli blocking weights and no Coulomb interaction.

The experimental spectrum of the compound system, ^{7}He, and theoretical spectra where target state widths are considered and set to zero are displayed in Fig. 10. Again, as the parameters are tuned to the no-widths case (published in
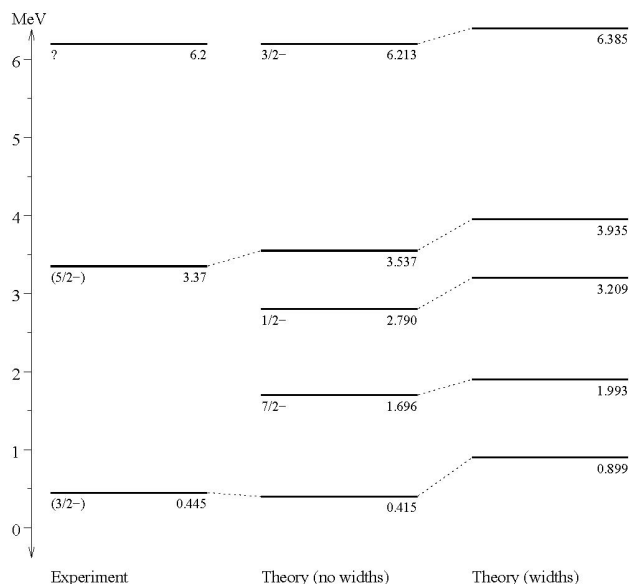
FIGURE 10. Experimental ^{7}He spectrum and those from (no widths and widths) MCAS calculations of the $n+^6$He system.

Ref. 12 and shown here for comparison with the new widths calculation), this appears first after experiment. Also, as no positive parity states are known, no positive parity interaction was used in these calculations.

In this case there is much movement of resonance centroids when the target states are taken to be resonances themselves. The trend, though, is as found in the previous studies. Likewise the low energy cross section (not depicted) has a similar asymptotic increase as energy tends to zero as evident in the $n+^8$Be case. This is further evidence a more sophisticated method is required to prevent width-penetration into the negative energy regime, one in which the influence of target states widths approaches zero as projectile energy approaches zero.

8. Discussion and conclusions

An extension to MCAS that considers particle-decay widths of target nucleus eigenstates has been further tested for a range of light mass nuclear targets. A Heaviside step function has been applied to those target state widths when used in the energy denominators of the coupled-channel Lippmann-Schwinger equations. This ensures that the Lorentzian shape of the target state resonances has no effect below threshold ($E = 0$) which would compromise stability in the compound bound system.

Experimental cross section data at 147° for $p+^{14}$O scattering has been compared with previously published results. Inclusion of defined target state widths gives only a marginally better representation of resonance magnitudes in the cross section. Using target state widths five times the

known size brings the larger $\frac{5}{2}^+$ resonance into agreement with experiment.

In addition to evidence supporting previous findings that consideration of target state widths increase the calculated widths of elastic cross section resonances, and that at low energy, the centroids of such are little altered, new trends have been found. First, when comparing results of calculations that include target state widths to those from calculations that do not, the compound nucleus spectrum, generally, will be wider spread with most centroids increasing with excitation energy. This phenomenon is evident in the investigations of the $n+^8$Be, of the $p+^8$Be, of the $p+^6$He, and especially of the $n+^6$He systems. The effect seems to increase as target state widths increase.

To ensure that any resonance aspect of target states does not have influence below the nucleon-nucleus threshold in our formalism, we have used a Heaviside function in the specification of the coupled-channel Green's function. This, however, is too simplistic. A first problem with the approach occurs with specification of compound states that lie near to the threshold energy. In the case of the ^{9}Be spectrum, a very weakly bound state was found with the no-width calculation which became a resonance with very low centroid energy upon allowing the target states to be resonances with Lorentzian character. The Heaviside weighting, however, retains the state as a weakly bound one. This problem is caused in the current formalism as the effect of a target width is felt for all positive values of projectile energy, the Lorentzian never having a zero value. A better energy dependent scaling factor is needed; one with value one at the centroid energy and approaching zero for lower and higher energies faster than a Lorentzian. Another problem with the current model is that reaction cross sections increase asymptotically as the projectile energy tends to zero. New investigations will see if that undesirable effect can be offset with a more appropriate energy dependent scaling factor applied to the target state

A further problem of the current formalism, one not observed previously [7], is that at the larger excitation energies, use of target state widths can change the calculated spectrum of the compound system significantly. Our $p+^{14}$O and $p+^6$He studies showed that. Hence when allowing target states to be resonances themselves, the nuclear interactions deemed best from a no-width study may need adjustment in concert with the specification of target state resonances.

Acknowledgments

1. K. Amos *et al.*, *Adv. Nucl. Phys.* **25** (2000) 275.

2. A. Lagoyannis *et al.*, *Phys. Lett. B* **518** (2001) 27.

3. S.V. Stepantsov *et al.*, *Phys. Lett. B* **542** (2002) 35.

4. D. Ridikas *et al.*, *Nucl. Phys. A* **628** (1998) 363.

5. K. Amos *et al.*, *Nucl. Phys. A* **728** (2003) 65.

6. P.R.S. Gomes *et al.*, *Nucl. Phys. A* **828** (2009) 233.

7. P. Fraser *et al.*, *Phys. Rev. Lett.* **101** (2008) 242501.

8. S. Weinberg, in *Lectures on Particles and Field Theory, Vol. Brandeis Summer Institute in Theoretical Physics* vol 2. (Prentice-Hall, 1965) p. 289.

9. L. Canton *et al.*, *Phys. Rev. Lett.* **94** (2005) 122503.

10. K. Amos *et al.*, *Phys. Rev. C* **72** (2005) 064604.

11. L. Canton *et al.*, *Phys. Rev. Lett.* **96** (2006) 072502.

12. L. Canton *et al.*, *Phys. Rev. C* **74** (2006) 064605.

13. G. Cattapan, L. Canton, and G. Pisent, *Phys. Rev. C* **43** (1991) 1395.

14. D.R. Tilley *et al.*, *Nucl. Phys. A* **745** (2004) 155.

15. I. Mukha *et al.*, *Phys. Rev. C* **79** (2009) 061301(R).

16. V.Z. Goldberg *et al.*, *Phys. Rev. C* **69** (2004) 031302(R).